

PRENATAL DEVELOPMENT OF SKULL AND BRAIN IN A MOUSE MODEL OF GROWTH RESTRICTION

Jimena Barbeito-Andrés^{1,2*}, Paula N. Gonzalez^{1,2}, Benedikt Hallgrímsson³

¹ Facultad de Ciencias Naturales y Museo. Universidad Nacional de La Plata. La Plata. Buenos Aires. Argentina

² Instituto de Genética Veterinaria "Ing. Fernando N. Dulout". Universidad Nacional de La Plata - CONICET. Buenos Aires. Argentina

³ Department of Cell Biology and Anatomy. McCaig Institute for Bone and Joint Health. University of Calgary. Calgary. Alberta. Canada

KEY WORDS maternal protein restriction; phenotypic integration; cranial modules; micro-CT

ABSTRACT Patterns of covariation result from the overlapping effect of several developmental processes. By perturbing certain specific developmental processes, experimental studies contribute to a better understanding of their particular effects on the generation of phenotype. The aim of this work was to analyze the interactions among morphological traits of the skull and the brain during late prenatal life (18.5 days postconception) in mice exposed to maternal protein undernutrition. Images from the skull and brain were obtained through micro-computed tomography and 3D landmark coordinates were digitized in order to quantify shape and size of both structures with geometric morphometric techniques. The results highlight a systemic effect of protein restriction on the size of the skull and the brain, which were both significantly reduced in the undernourished group compared to control group. Skull shape

is partially explained by brain size, and patterns of shape variation were only partially coincident with previous reports for other ontogenetic stages, suggesting that allometric trajectories across pre- and postnatal ages change their directions. Within the skull, neurocranial and facial shape traits covaried strongly, while subtle covariation was found between the shape of the skull and the brain. These findings are in line with former studies in mutant mice and reveal the importance of carrying out analyses of phenotypic variation in a broad range of developmental stages. The present study contributes to the basic understanding of epigenetic relations among growing tissues and has direct implications for the field of paleoanthropology, where inferences about brain morphology are usually derived from skull remains. *Rev Arg Antrop Biol* 18(1), 2016. doi:10.17139/raab.2016.0018.01.05

PALABRAS CLAVE restricción proteica materna; integración fenotípica; módulos craneanos; micro-TC

RESUMEN Los patrones de covariación entre rasgos fenotípicos resultan de la acción de diversos procesos que se solapan durante el desarrollo. Los estudios experimentales constituyen la aproximación más adecuada para evaluar el efecto de procesos específicos en la generación de tales patrones. El objetivo de este trabajo es analizar las interacciones entre rasgos morfológicos craneofaciales y cerebrales durante la vida prenatal tardía (18,5 días posconcepción) en ratones expuestos a desnutrición proteica materna. Se obtuvieron imágenes del cráneo y cerebro a partir de microtomografía computada y se digitalizaron landmarks en 3D para cuantificar la forma y tamaño con técnicas de morfometría geométrica. Los resultados subrayan un efecto sistémico de la restricción proteica en el tamaño del cráneo y el cerebro. La forma del cráneo es parcialmente explicable por el tamaño cerebral y

los patrones de variación en forma fueron sólo en parte coincidentes con los reportados antes para otras edades, lo cual sugiere que las trayectorias alométricas a lo largo de la vida pre- y posnatal cambian su dirección. Los rasgos de forma del neurocráneo y el esqueleto facial covariaron fuertemente, aunque se encontró una asociación débil entre la forma del cráneo y del cerebro. Estos resultados concuerdan con estudios previos en ratones mutantes y revelan la relevancia de analizar la variación fenotípica en distintas etapas. El presente estudio contribuye al conocimiento básico de las interacciones epigenéticas entre tejidos en crecimiento y tiene implicancias en el campo paleoantropológico en el que las inferencias acerca de la morfología cerebral son usualmente derivadas del análisis del cráneo. *Rev Arg Antrop Biol* 18(1), 2016. doi:10.17139/raab.2016.0018.01.05

The mammalian skull comprises several heterogeneous osseous structures that dynamically interact with one another as well as with the surrounding organs and tissues. The neurocranium, which can be further divided into vault and basicranium, and the face have been widely recognized to form the main modules of the skull, on the basis of their developmental and functional differences (Cheverud, 1982, 2007; Enlow and Hans, 1998; Sperber, 2001). Despite these dissimilarities, several growth

Funding: This study was supported by the AAPA Professional Development Program. The CIHR Training Program in Genetics, Child Development and Health (Alberta Children's Hospital) and grants from AIHS to PG. NIH 1R01DE021708 and 1R01DE01963, and NSERC #238992-12 to BH.

*Correspondence to: Dra. Jimena Barbeito-Andrés. Facultad de Ciencias Naturales y Museo. Universidad Nacional de La Plata. 60 y 122. 1900 La Plata. Buenos Aires. Argentina. E-mail: barbeito@fcnym.unlp.edu.ar

Recibido 19 Noviembre 2014; aceptado 10 Marzo 2015

doi:10.17139/raab.2016.0018.01.05

factors and genes with pleiotropic effects on neurocranial and facial morphogenesis (Helms et al., 2005; Tapiada et al., 2005), as well as the epigenetic interactions between both regions, contribute to keeping the skull structurally and functionally coherent (Richtsmeier et al., 2006; Hallgrímsson et al., 2007; Mitteroecker and Bookstein, 2008). By epigenetic interactions we refer here to the wide-ranging set of developmental mechanisms, such as physical interactions, that take place in particular spatiotemporal contexts where cells, tissues and organs develop and function (Hallgrímsson and Hall, 2011). As a phenotypic result of such developmental dynamics, covariation between neurocranial and facial traits has been consistently found in different mammals, including primates (Bookstein et al., 2003; Martínez-Abadías et al., 2011; Singh et al., 2012), although the relative independence of skull modules seems to be variable among species (Polanski and Franciscus, 2006; Marroig et al., 2009).

Among the processes that generate covariation of morphological traits in the skull, brain growth has been largely considered one of the most influential throughout early to postnatal ontogeny (Moss and Young, 1960; Opperman, 2000; Richtsmeier et al., 2006; Richtsmeier and Flaherty, 2013). The developmental link between skull and brain becomes evident from medical disorders that affect the morphogenesis of both structures jointly (Cohen et al., 1992; Aldridge et al., 2002, 2005a, b, 2007). Some examples include anencephaly, in which brain absence relates to abnormal formation of vault bones (Dambaska et al., 2003; Davies and Duran, 2003; Frey and Hauser, 2003), and hydrocephaly, characterized by an excessive accumulation of cerebrospinal fluid that increases neurocranial size (Morimoto et al., 2003). Recent studies have described epigenetic mechanisms, including physical interactions and molecular signaling of embryonic brain tissues on craniofacial structures, that account for the early and close relation between the brain and facial prominences (Boughner et al., 2008; Marcucio et al., 2011; Richtsmeier and Flaherty, 2013). From an evolutionary perspective, this is relevant because some aspects of the human skull, such as the unusually flexed basicranium and the orthograde face, have been interpreted as a re-

sponse to structural demands of the expanding brain (Lieberman et al., 2008).

In recent years, much interest has been devoted to the similarity in patterns of morphological covariation across species and ontogenetic stages within species (e.g. Ackermann and Cheverud, 2000; Ackermann, 2005; Mitteroecker and Bookstein, 2009; Willmore et al., 2009), as well as to the developmental processes that produce them. Because the observed patterns result from the overlapping effect of several processes along ontogeny, the developmental determinants of covariation can only be explored by means of experimental designs that introduce variation by perturbing specific processes (Hallgrímsson et al., 2009). For the case of the mammalian skull, mice represent the most widely studied model. So far, the work on this topic has focused on the effect of genetic mutations related to noticeable dysmorphologies, such as craniosynostosis and altered brain growth (Aldridge et al., 2005a, b, 2010), and on the analysis of very early prenatal (Boughner et al., 2008; Marcucio et al., 2011) and postnatal stages (Hill et al., 2013).

Here, we assess the morphological association between cranial structures and the brain during late prenatal life by altering somatic growth, a key developmental process that generates covariation among traits. In order to achieve this goal, mouse embryos were exposed to maternal undernutrition, an environmentally induced perturbation with well documented effects on cranial growth (Pucciarelli and Goya, 1983; Pucciarelli and Oyhenart, 1987; Pucciarelli, 1991; Oyhenart et al., 1994; Cesani et al., 2006; Gonzalez et al., 2011a). Particularly, we analyze brain and skull phenotypes in mouse fetuses at E18.5 from an experimental model of maternal undernutrition to assess: a) the association between skull shape and brain size; b) coordinated shape variation between the skull and the brain as well as the allometric effect on their covariation; and c) coordinated shape changes between the neurocranium and the face, and the allometric effect on their covariation. This prenatal stage was chosen because it constitutes a temporal point at which the specimens are relatively advanced in their ossification, but masticatory dynamics and other functional factors have not yet exerted their influence, and thus, their effect

on the pattern of association among craniofacial traits can be ruled out.

MATERIAL AND METHODS

Sample and data acquisition

C57BL/6J male and female 4-wk-old mice were purchased from The Jackson Laboratory (Bar Harbor, ME) and maintained on a 12-h light/12-h dark cycle for 4 weeks. During this period they were fed on a control diet (20% protein TD91352, Harlan Teklad, Madison). Then, non-sibling females were randomly divided into two groups, Control (CG) and Low Protein (LPG), which received isocaloric diets (3.8 Kcal/g) that differed in the amount of protein, 20% and 6% (TD90016, Harlan Teklad, Madison), respectively. After two weeks of receiving these diets, breeders were placed together overnight until vaginal plugs were detected. Pregnant females were maintained with the assigned diet (6% or 20% protein) until 18.5 days postconception (E18.5). At that point pregnant females were sacrificed and the conceptuses were removed. The samples were composed as follows: Control Group (CG), composed of 40 fetuses from 9 litters whose mothers received 20% protein diet throughout pregnancy; Low Protein Group (LPG), composed of 31 fetuses from 6 litters whose mothers received the 6% protein diet. All animal procedures were reviewed and approved by the University of Calgary Health Sciences Animal Care Committee and experiments were conducted in compliance with this approval. Animals were cared for as per the guidelines of the Canada Council on Animal Care.

The skulls of fetuses from both control and restricted protein groups were fixed overnight in 4% phosphate-buffered formaldehyde and then imaged using a micro-CT scanner (μ CT 35, Scanco Medical AG, Brüttsellen, Switzerland). The specimens were scanned using the same parameters: isotropic voxel size of 0.012mm, 45kVp, 177 μ A, 800000 ms integration time and 500 projections per 180 degrees. The 2D images of the skull were rendered into 3D isosurfaces in Amira 5.2.2 (Visualization Science Group) using a threshold of 3500 Hounsfield units. A subsample of specimens was treated with iodine 2% in order to stain the soft tissues (Metscher,

2009). Briefly, 0.5g of iodine and 1.5g of potassium iodide were mixed in 98mL of water; heads were immersed in the iodine solution and kept at 4C overnight. Then, the samples were rinsed in PBS to remove the excess of contrast agent and scanned using the same parameters as for the skull. This simple contrast staining technique is a valid alternative to the magnetic resonance images commonly applied to the study of the brain in lab animals, at least for the description of its external morphology.

Shape and size were quantified by means of 3D landmark coordinates of the skull and brain obtained from micro-computed tomography images (micro-CT) and analyzed with geometric morphometric techniques. Micro-CT techniques are key in experimental research based on murine models because many morphological aspects are not easily observable with other 2D tools, such as photography or radiography. This is especially important for the examination of prenatal specimens, as those analyzed here, which requires high levels of resolution and the use of precise protocols to gain access to bone and soft structures (Nieman et al., 2012). From the 3D reconstruction of each mouse cranium, 21 landmarks were digitized on the skull and a set of 11 landmarks was digitized on the micro-CT scans of the brain (Table 1, Fig. 1). Only the right side of both configurations, brain and skull, were digitized. The cranial landmarks were chosen to describe the face, base and vault, previous studies on neonatal mice (Boughner et al., 2008; Martinez-Abadías et al., 2011). However, because of the low degree of ossification of parietal, temporal and occipital bones at the prenatal stage studied here, some of the proposed landmarks were not observable. Brain landmarks were chosen to describe main variation in overall brain proportions, as well as the relative size of the olfactory bulb and the cerebellum. In general, the relation between sample sizes and number of landmarks is comparable with other experimental studies on the topic that are discussed herein.

Statistical analyses

Centroid size (CS) of the skull and the brain was estimated as the square root of the summed squared distances from all landmarks to the cen-

TABLA 1. List of 3D landmarks digitized on the skull and the brain

Landmark	Definition	Region
1	Most superior anterior point of the premaxilla	Face
2	Most posterior lateral point of the nasal bone	Face
3	Most superior posterior point of the premaxilla	Face
4	Intersection of frontal process of maxilla with frontal and lacrimal bones	Neurocranium
5	Most anterior lateral point of the frontal bone, taken close to the frontal process of maxilla	Neurocranium
6	Most lateral intersection of the frontal, parietal and squamous bones, taken on the frontal, left side	Neurocranium
7	Most lateral intersection of the frontal and parietal bones, taken on the frontal	Neurocranium
8	Most lateral intersection of the frontal and parietal bones, taken on the parietal	Neurocranium
9	Intersection of zygoma process of maxilla, taken on maxilla	Face
10	Intersection of zygoma process of maxilla, taken on zygoma	Face
11	Intersection of zygoma with zygomatic process of temporal, taken on zygoma	Face
12	Most anterior point on the anterior extension of the forming squamosal	Neurocranium
13	Most posterior point on the posterior extension of the forming squamosal	Neurocranium
14	Most anterior point of the anterior palatine foramen	Face
15	Most inferior-lateral point of the premaxillary-maxillary suture, taken on premaxilla	Face
16	Most anterior point of the posterior palatine foramen	Face
17	Posterior-medial point of the inferior portion of the left side of the aliesphenoid	Neurocranium
18	Most anterior-lateral point corner of the basioccipital	Neurocranium
19	Most posterior-lateral point corner of the basioccipital	Neurocranium
20	Point on the most medial point of the lateral occipital, in the hypoglossal canal	Neurocranium
21	Superior posterior point on the ectocranial surface of occipital lateralis on the foramen magnum	Neurocranium
1	Most posterior point in the intersection of cerebellar hemispheres, in the axial plane	Brain
2	Most posterior point in the intersection of olfactory lobes, in the axial plane	Brain
3	Most anterior point in the intersection of olfactory lobes, in the axial plane	Brain
4	Anterior-lateral point in the cerebral cortex in the intersection with olfactory lobes, in the axial plane	Brain
5	Most posterior point of the cerebral cortex in the intersection with cerebellum, in the axial plane	Brain
6	Inferior intersection of the midbrain and the pons	Brain
7	Most anterior point of olfactory lobe	Brain
8	Most anterior point of cerebral cortex in the intersection with olfactory lobe	Brain
9	Deepest point in the fold of the cerebral cortex	Brain
10	Deepest point in the dorsal sulcus of cerebellum	Brain
11	Deepest point in the ventral sulcus of cerebellum	Brain

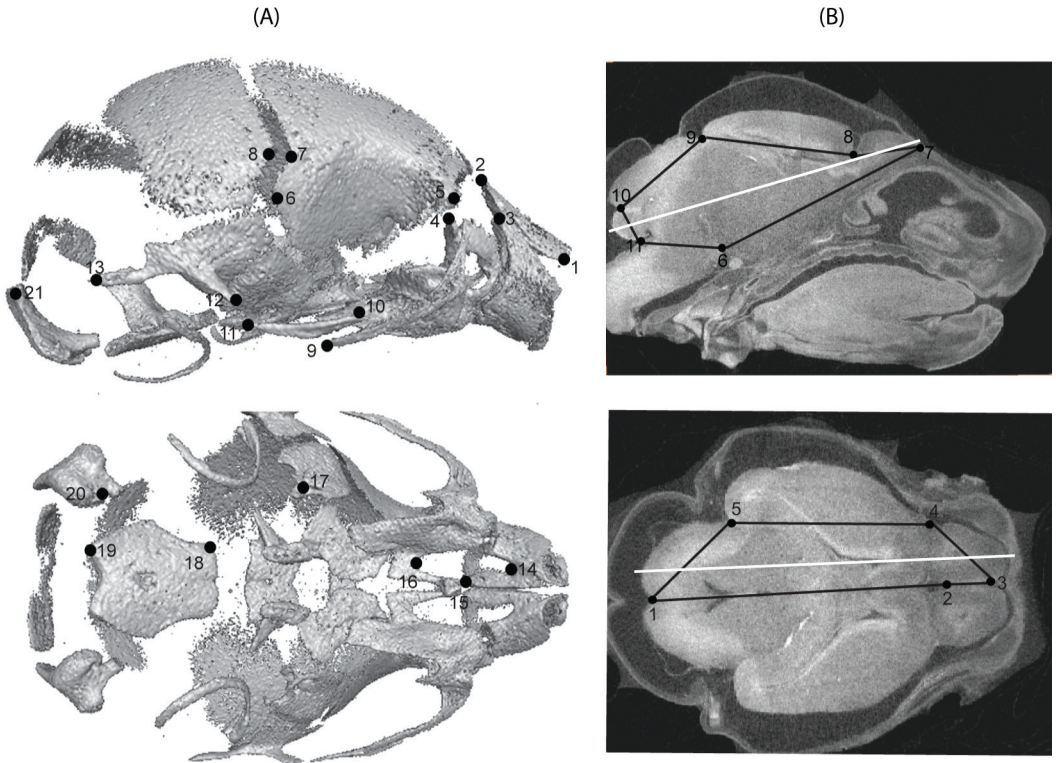


Fig. 1. Landmark coordinates of the skull (A) and the brain (B). In (B) landmarks were digitized in parasagittal and axial sections as indicated with white lines.

troid of each configuration (Bookstein, 1997). Estimated measures of size were compared across treatments by means of a mixed model ANOVA, using treatment as a fixed effect and dam as a random effect.

Landmarks were superimposed by means of Generalized Procrustes Superimposition (GPS) in order to obtain shape coordinates. Through this procedure landmark coordinates were translated, rotated and scaled using a least-squares superimposition until they were optimally aligned (Rohlf and Slice, 1990). To analyze the association between skull shape and brain size a multivariate regression of Procrustes coordinates of the skull on log-transformed CS of the brain (log CS Brain) was performed (Monteiro, 1999). The regression model accounts for an amount of variation that is measured as a percentage of total shape variation (Klingenberg and McIntyre, 1998). Statistical significance of the regressions was assessed through permutation tests against the null hypothesis of inde-

pendence. Visual resources were used to depict the patterns of size-related shape changes in the skull. 3D morphings of the whole skull were obtained using the thin-spline procedure implemented by Landmark software (Wiley et al., 2005).

Coordinated shape variation between sets of landmarks representing different anatomical structures was assessed using two-block Partial Least Squares (PLS) analysis. GPS was performed separately for each block of landmarks in PLS analyses. PLS is based on singular value decomposition of the covariance matrix and results in new pairs of axes that account for maximum covariation between these previously defined blocks (Rohlf and Corti, 2000; Bookstein et al., 2003). To quantify the strength of covariation between parts, we used the RV coefficient, which quantifies the total covariation as the sum of all squared covariances between blocks (Klingenberg, 2009), and also the correlation coefficient among PLS scores (Rohlf and Corti, 2000).

Here, PLS analyses were carried out for the whole skull and the brain, as well as for the neurocranium and the face. In the first case, as in all analyses that involved the brain, only those specimens belonging to the brain-stained subsample were used ($n=18$), whereas in the latter all the specimens were included ($n=71$). Patterns of shape covariation in the skull were depicted by 3D morphings obtained in Landmark software, while changes in the brain were visualized by means of wireframes (Klingenberg, 2013).

In order to account for the allometric effect on covariation, PLS analyses were repeated using the residuals of the multivariate regression of Procrustes coordinates on the CS of each region. These new analyses were based on the shape variation that was not predicted by the regression model and, therefore, represented covariation between regions once size effect has been controlled (Monteiro, 1999; Klingenberg, 2009; Martínez-Abadías et al., 2011).

RESULTS

According to our results, mean skull CS was 4.96% lower in LPG than in CG ($F=4.943$, $p<0.0001$) (Fig. 2). In both skull modules CS was larger in CG; in the neurocranium the difference reached 5.07% ($F=8.926$, $p<0.0001$), while in the face it was 4.88% ($F=7.613$, $p<0.0001$). The

same trend was found for the brain CS, where a difference of 4.94% was found between groups ($F=6.582$, $p=0.021$) (Fig. 2). This similarity is in line with the finding of a significant correlation between skull and brain CS using Pearson correlation coefficient (0.732 , $p<0.001$).

Multivariate regression analysis computed with Procrustes coordinates of the whole skull on brain log-transformed CS showed that brain size variation explained 10.69% ($p=0.047$) of shape variation in the skull. A subtle separation was found in the distribution between CG and LPG (Fig. 3). At the positive extreme (bigger brains), skull configurations are narrower in the facial segment and in the vault, while the basioccipital bone is wider (Fig. 3). The specimens at this extreme are also characterized by flexed skulls and projected faces, as is shown in the lateral view (Fig. 3).

Shape covariation between the brain and the whole skull was assessed through PLS using Procrustes coordinates of the brain and the skull. The first pair of PLS (PLS1) explains 49.33% of the total covariance. Although the relation explained by the PLS1 was not significant (and no other PLS resulted significant), some tendencies in coordinated variation among the two blocks can be described. For PLS1, negative scores were mainly occupied by the CG specimens (Fig. 4), and skulls were narrower;

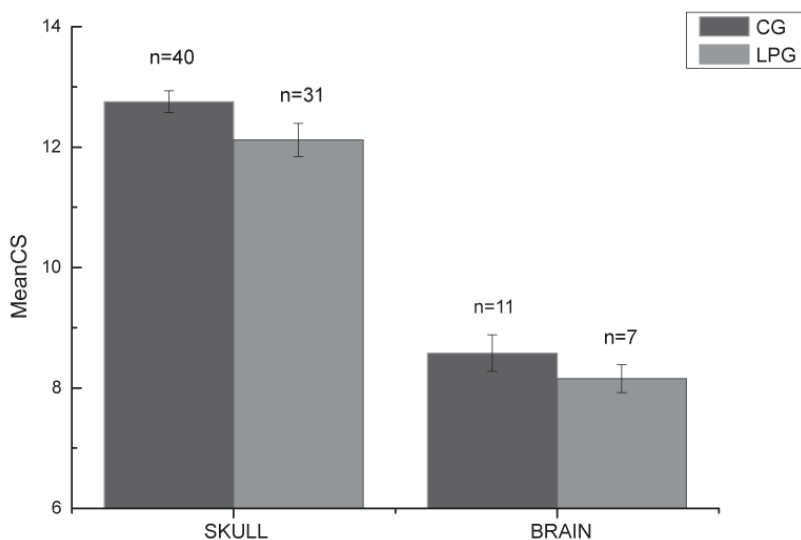


Fig. 2. Mean centroid size (MeanCS) of the skull and the brain. Error bars show standard deviations.

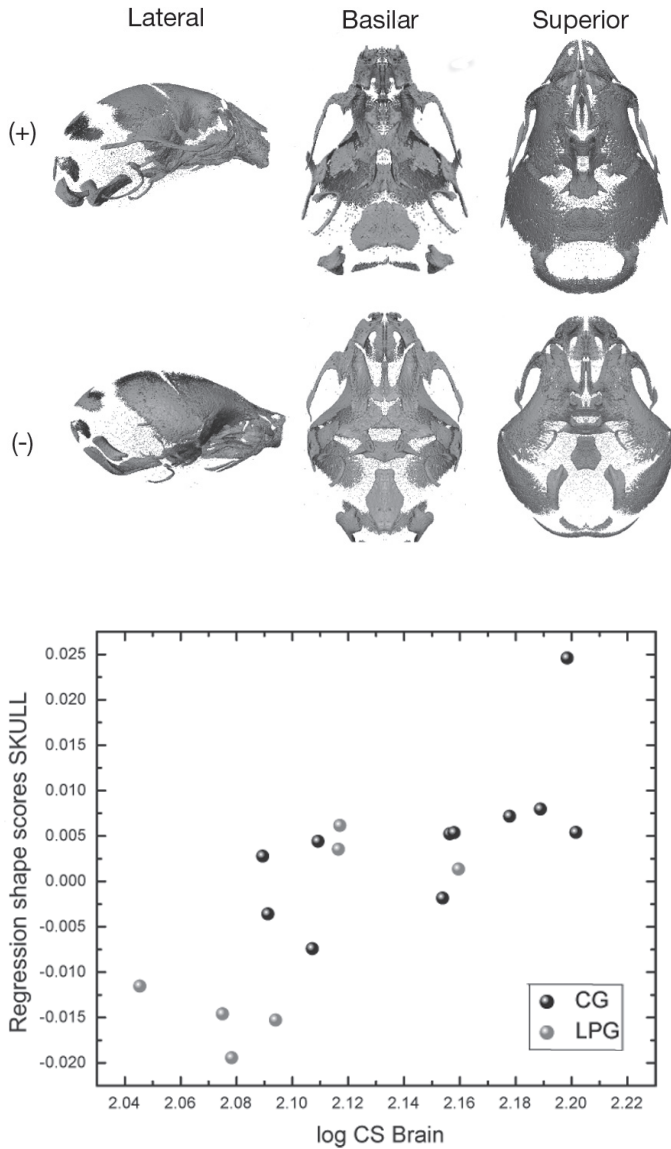


Fig. 3. Multivariate regression of skull Procrustes coordinates on log CS Brain. Morphings represent the shape changes for extreme negative and positive scores.

the neurocranium was flexed in the base covarying with vertically shorter brains (Fig. 4). At the positive extreme of the distribution, the skull was wider and the anterior face was in line with the anterior-posterior axis of the skull. This skull configuration covaried with taller brains (Fig. 4). PLS analysis between the brain and the skull was carried out after adjusting size variation, and the PLS1 explained 36.44% of covaria-

tion, although the overall strength of association between blocks was low (RV coefficient=0.340, $p=0.5235$).

Finally, two-block PLS analysis between the neurocranium and the face indicated that these regions covaried strongly. The first PLS axis accounts for 60.29% of the total squared covariance. Although distribution of CG and LPG specimens along the first pair of PLS axis is

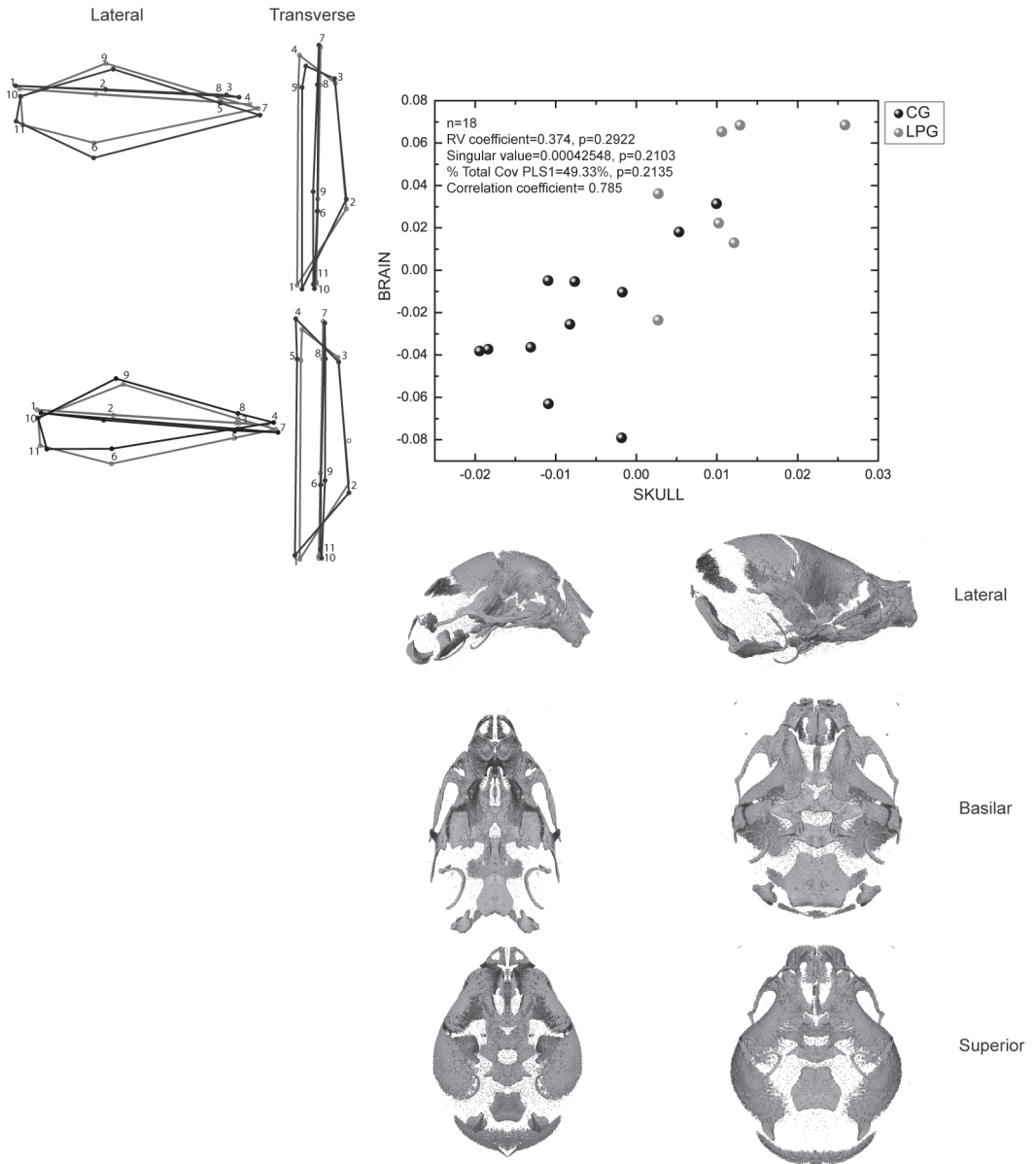


Fig. 4. PLS1 of the skull vs. the brain and visualizations of coordinated shape changes.

partially overlapping, the latter tend to occupy negative scores, while CG are placed at positive scores (Fig. 5). At the negative scores (LPG), short and wide faces covary with a particular configuration in the neurocranium: parietal and occipital regions are wide, while frontal bones tend to converge towards the sagittal line. At the positive extreme (CG), antero-posteriorly long and narrow faces covary with narrow pa-

rietal and occipital bones, while frontal bones (especially in the most anterior segment) open laterally and widen. From a lateral view it can be noticed that taller faces were linked to a taller neurocranium for the positive scores, while the opposite configurations were found among specimens that occupied negative scores (Fig. 5). Neurocranium CS explained 13.28% ($p < 0.0001$) of its shape variation, while face

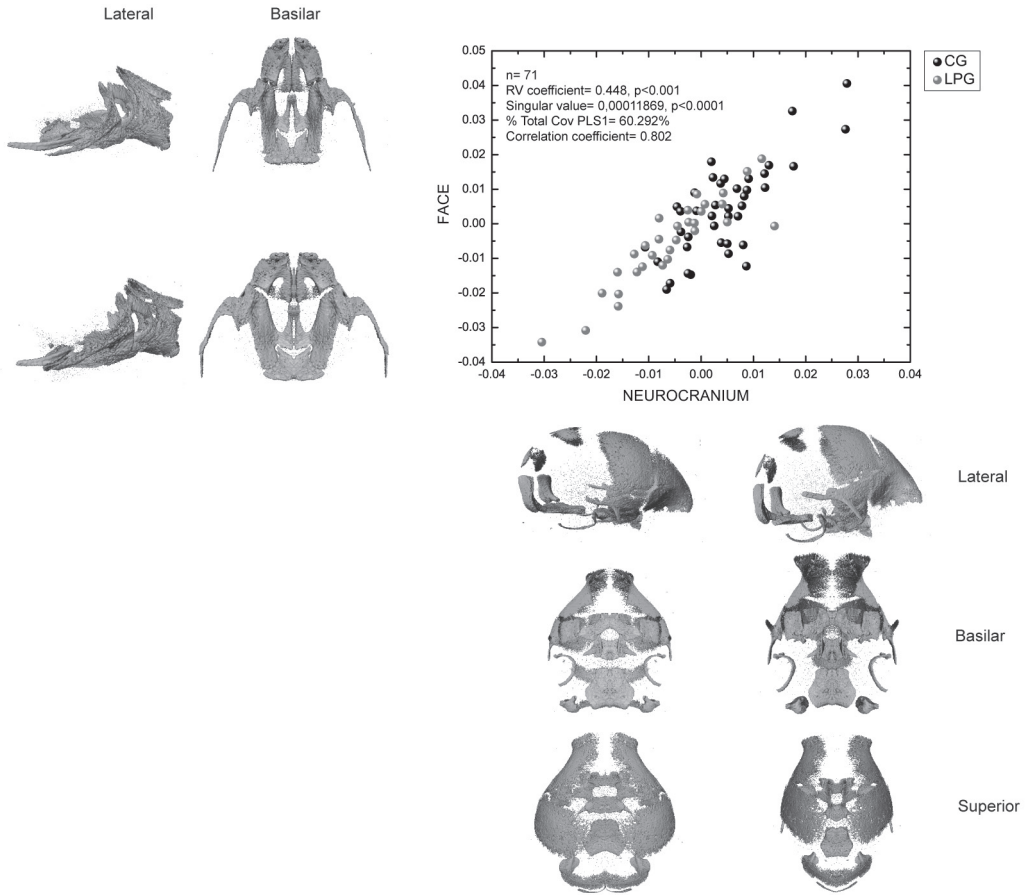


Fig. 5. PLS1 of the neurocranium vs. the face and visualizations of coordinated shape changes.

CS accounted for 16.18% ($p < 0.0001$) of shape variation. When PLS between the neurocranium and the face was carried out using the residuals of these multivariate regressions of Procrustes coordinates on CS, the covariation explained by PLS1 decreased only slightly (PLS1=54.013%, RV coefficient=0.323, $p < 0.0001$).

DISCUSSION

Our results indicate that chronic protein restriction during gestation significantly reduces brain and cranial growth by the end of the fetal period. They also show that size changes in both structures are strongly associated. Because the environmental perturbation studied here has a systemic effect on organism growth, the association between brain and skull might result from correlated responses to nutrient restriction

rather than from the direct influence of one on the other. It has been proposed that generalized changes in size usually affect different parts of an organism jointly and therefore produce a global increase in covariation among traits (Chernoff and Magwene, 1999; Klingenberg, 2009; Gkantidis and Halazonetis, 2011). However, studies in rodents and other model organisms show that plasticity of individual organs can be distinct, displaying partly independent responses to the same environmental factors that regulate size (Shingleton et al., 2009; Gonzalez et al., 2011a). Evidence of semi-autonomous changes in the brain and skull is also provided by mutant mice. Models for Apert syndrome, for example, show that both structures display a relative dissociation in their size at early postnatal stages, which is interpreted in terms of stronger effects of the mutation on the skull than on the brain

(Hill et al., 2013). According to our results, the environmental perturbation induced here has a similar effect on prenatally growing brain and skull size, showing the generalized effect of maternal malnutrition on these tissues.

Brain size was also significantly associated with skull shape, accounting for 10.69% of this variation. Although this proportion is relatively low, it is comparable to earlier estimates from intraspecific analyses of static allometry of different species, such as humans and dogs, in the context of geometric morphometric studies (Drake and Klingenberg, 2008; Gonzalez et al., 2011b). The pattern of changes associated with larger brains was characterized by a relatively wider cranial base, longer antero-posterior axis, and flexed cranial bases compared to specimens with smaller brains (Fig. 5). In an experimental study on adult mutant rodents with megalencephalic phenotypes, Lieberman et al. (2008) found that an increase in brain size is related to particular skull shape changes, such as antero-posteriorly longer and vertically taller neurocranium, as well as to a more flexed base. Although these patterns seem to be congruent with our findings, there are others that reported different interactions between brain size and craniofacial morphology in mice and other mammalian species. While we found that by E18.5 mouse faces tend to be projected and relatively larger in configurations with larger brains, for very early prenatal stages Boughner and collaborators (2008) showed that more prognathic faces are characteristic of shorter developing brains in mice. As another example, in a study on human adult skulls Martínez-Abadías et al. (2012) described wider vaults and shorter vertically oriented faces corresponding to larger brains, while contrasting trends were found here for these traits (Fig. 5). Although that work on humans is framed in a quantitative genetics approach and, consequently, direct comparisons may not be valid, it provides some basis for the discussion of our results with findings on human morphology in another developmental stage. The discrepancies between some shape changes observed here and the tendencies showed in previous studies could stem from differences in the developmental stages analyzed. Several works have documented that morphogenesis of mammalian skull is characterized by changes in the

direction of allometric trajectories across pre- and postnatal ages, and by the nonlinearity of shape changes (Zelditch, 2003; Gonzalez et al., 2011b). Patterns of covariation among morphological traits are restructured during ontogeny, as different developmental processes influence them. Therefore, differences in the structure of association among traits between successive age stages are the result of the superimposition of novel covariance patterns. Analyses of age-specific morphological variation and covariation, and comparisons with other stages are essential to infer the ontogenetic timing and the phenotypic effects of developmental processes such as brain growth (Mitteroecker and Bookstein, 2009).

Contrary to the pattern observed for size variables, a relatively weak association between brain and skull shape was found, as is shown by the PLS analysis performed on Procrustes shape coordinates. Along the first axis of covariation, a narrower and flexed neurocranium is associated with a vertically shorter brain. After studying a model for craniosynostosis, Aldridge et al. (2010) concluded that the processes underlying alterations of the vault are relatively independent from those causing brain dysmorphologies. Hill et al. (2013) also found a non-significant correlation between brain and skull morphology in mice at the time of birth, which is an ontogenetic stage very close to the late prenatal day analyzed in our study. However, they noted that this trend is altered in the immediately following days and two days after birth, when skull and brain morphology correlate significantly. Similarly, a tight fit of the brain and skull size and shape was documented in adult mice carrying mutations that affect brain development (Nieman et al., 2012). This further reveals the occurrence of significant changes in the patterns of morphological covariation during the early stages of skull development.

When covariation between the shape of the neurocranium and the face was examined, we found shape changes that resemble those described for the regression of skull shape on brain size analysis. Wider and vertically shorter facial skeletons were associated to posteriorly wider vaults, while antero-posteriorly longer and vertically taller faces correspond to

a longer neurocranium (Fig. 4). However, there are some relevant shape changes, for instance, basicranial flexion, that were not observed in the PLS analysis for the neurocranium and the face. Previous studies have described that the flexion of the base is particularly related to brain expansion in size (Hallgrímsson and Lieberman, 2008). This is in line with our results, since changes in base flexion were found only when the brain was considered in the analysis. Coordinated variation between the neurocranium and the face is restricted to relative length, height, and width changes of both structures, but base flexion seems to be independent of their association.

In conclusion, our results indicate that alterations in fetal growth produce coordinated changes of skull shape and size with brain size, while brain shape variation is not tightly associated with skull shape. These findings are in agreement with previous studies in mutant mice and reinforce the relevance of performing more complete analyses of phenotypic variability in response to genetic and environmental factors in a broader range of developmental stages. Regarding this point, possible differential responses to dietary perturbations in different mouse strains have not been deeply analyzed. Although some studies have found variations in certain physiological parameters when mouse lines were compared (e.g. Radiloff et al., 2008; La Merrill et al., 2010), morphological phenotypes, as analyzed in this study, are expected to behave differently. Developmental processes intervening in morphological differentiation are limited in number and tend to be more conservative (Hallgrímsson and Lieberman, 2008). In support of this expectation, patterns of craniofacial morphological variation similar to those found here were observed in rats under comparable treatments of maternal malnutrition (Gonzalez et al., 2011c; Martínez-Abadías et al., 2012). Consequently, although more work is necessary, it is plausible that our results can be extrapolated at least to other murine models.

In addition to its significance for a deeper understanding of epigenetic interactions between growing tissues, the relationship between the brain and the skull is of interest for anthropological and evolutionary studies. In this context, in-

ferences about brain evolution are based on evidence of skull shape, which is more commonly preserved in the fossil record, and, therefore, they rely on the assumption that endocranial reconstructions are a good proxy for brain features (Bruner, 2004; Neubauer et al., 2010; Gunz et al., 2012). Experimental designs with animal models, as the one performed here, can contribute to evaluating under which circumstances and to what extent these assumptions are valid.

ACKNOWLEDGMENTS

We thank Heather Jamniczky and Tegan Barry for their help with the protocols for brain staining. We also thank two anonymous reviewers for their insightful suggestions.

LITERATURE CITED

- Ackermann RR. 2005. Ontogenetic integration of the hominoid face. *J Hum Evol* 48:175-197. doi:10.1016/j.jhevol.2004.11.001
- Ackermann RR, Cheverud JM. 2000. Phenotypic covariance structure in tamarins (genus *Saguinus*): A comparison of variation patterns using matrix correlation and common principal component analysis. *Am J Phys Anthropol* 111:489-501. doi:10.1002/(SICI)1096-8644(200004)111:4<489::AID-AJPA5>3.0.CO;2-U
- Aldridge K, Hill CA, Austin JR, Percival C, Martínez-Abadías N, Neuberger T, Wang Y, Jabs EW, Richtsmeier JT. 2010. Brain phenotypes in two FGFR2 mouse models for Apert syndrome. *Dev Dyn* 239:987-997. doi:10.1002/dvdy.22218
- Aldridge K, Kane AA, Marsh JL, Panchal J, Boyadjiev SA, Yan P, Govier D, Ahmad W, Richtsmeier JT. 2005a. Brain morphology in nonsyndromic unicoronal craniosynostosis. *Anat Rec A Discov Mol Cell Evol Biol* 285:690-698. doi:10.1002/ar.a.20201
- Aldridge K, Kane AA, Marsh JL, Yan P, Govier D, Richtsmeier JT. 2005b. Relationship of brain and skull in pre- and postoperative sagittal synostosis. *J Anat* 206:373-385. doi:10.1111/j.1469-7580.2005.00397.x
- Aldridge K, Marsh JL, Govier D, Richtsmeier JT. 2002. Central nervous system phenotypes in craniosynostosis. *J Anat* 201:31-39. doi:10.1046/j.1469-7580.2002.00074.x
- Aldridge K, Reeves RH, Olson LE, Richtsmeier JT. 2007. Differential effects of trisomy on brain shape and volume in related aneuploid mouse models. *Am J Med Genet A* 143:1060-1070. doi:10.1002/ajmg.a.31721
- Bookstein FL. 1997. *Morphometric tools for landmark data: geometry and biology*. Cambridge: Cambridge University Press.
- Bookstein FL, Gunz P, Mitteroecker P, Prossinger H, Schaefer K, Seidler H. 2003. Cranial integration in Homo: singular warps analysis of the midsagittal plane in ontogeny and evolution. *J Hum Evol* 44:167-187. doi:10.1016/S0047-2484(02)00201-4
- Boughner JC, Wat S, Diewert VM, Young NM, Browder LW, Hallgrímsson B. 2008. Short-faced mice and

- developmental interactions between the brain and the face. *J Anat* 213:646-662. doi:10.1111/j.1469-7580.2008.00999.x
- Bruner E. 2004. Geometric morphometrics and paleoneurology: brain shape evolution in the genus *Homo*. *J Hum Evol* 47:279-303. doi:10.1016/j.jhevol.2004.03.009
- Cesani MF, Orben AB, Oyhenart EE, Zucchi M, Muñe MC, Pucciarelli HM. 2006. Effect of undernutrition on the cranial growth of the rat. An intergenerational study. *J Anat* 209:137-147. doi:10.1111/j.1469-7580.2006.00603.x
- Cheverud JM. 1982. Phenotypic, genetic and environmental morphological integration in the cranium. *Evolution* 36:499-516. doi:10.2307/2408096
- Cheverud JM. 2007. The relationship between development and evolution through heritable variation. *Novartis Found Symp* 284:55-65. doi:10.1002/9780470319390.ch4
- Chernoff B, Magwene PM. 1999. Morphological integration: forty years later. In: Olson EC, Miller RL, editors. *Morphological integration*. Chicago: University of Chicago Press. p 319-353.
- Cohen MM, Kreiborg S, Lammer EJ, Cordero JF, Mastroiacovo P, Erickson JD, Roeper P, Martinez-Frias ML. 1992. Birth prevalence study of the Apert syndrome. *Am J Med Genet* 42:655-659. doi:10.1002/ajmg.1320420505
- Dambaska M, Schmidt-Sidor B, Maslinska D, Laure-Kamionowska M, Kosno-Kruszewska E, Deregowski K. 2003. Anomalies of cerebral structures in acranial neonates. *Clin Neuropathol* 22:291-295.
- Davies BR, Duran M. 2003. Malformations of the cranium, vertebral column, and related central nervous system: morphologic heterogeneity may indicate biological diversity. *Birth Defects Res A Clin Mol Teratol* 67:563-571. doi:10.1002/bdra.10080
- Drake AG, Klingenberg CP. 2008. The pace of morphological change: historical transformation of skull shape in St Bernard dogs. *Proc R Soc B* 275:71-76. doi:10.1098/rspb.2007.1169
- Enlow DH, Hans HM. 1998. *Crecimiento facial*. México DF: Mc-Graw Hill Interamericana.
- Frey L, Hauser WA. 2003. Epidemiology of neural tube defects. *Epilepsia* 44(Suppl 3):4-13. doi:10.1046/j.1528-1157.44.s3.2.x
- Gkantidis N, Halazonetis DJ. 2011. Morphological integration between the cranial base and the face in children and adults. *J Anat* 218:426-438. doi:10.1111/j.1469-7580.2011.01346.x
- Gonzalez PN, Perez I, Bernal V. 2011b. Ontogenetic allometry and cranial shape diversification among human populations from South America. *Anat Rec* 294:1864-1874. doi:10.1002/ar.21454
- Gonzalez PN, Oyhenart EE, Hallgrímsson B. 2011a. Effects of environmental perturbations during postnatal development on the phenotypic integration of the skull. *J Exp Zool* 314B:547-561. doi:10.1002/jez.b.21430
- Gonzalez PN, Hallgrímsson B, Oyhenart EE. 2011c. Developmental plasticity in covariance structure of the skull: effects of prenatal stress. *J Anat* 218:43-257. doi:10.1111/j.1469-7580.2010.01326.x
- Gunz P, Neubauer S, Golovanova L, Doronichev V, Maureille B, Hublin JJ. 2012. A uniquely modern human pattern of endocranial development. Insights from a new cranial reconstruction of the Neandertal newborn from Mezmaiskaya. *J Hum Evol* 62:300-313. doi:10.1016/j.jhevol.2011.11.013
- Hallgrímsson B, Hall BK. 2011. Epigenetics: the context of development. In: Hallgrímsson B, Hall BK, editors. *Epigenetics: linking the genotype and phenotype in development and evolution*. California: University of California Press. p 424-438.
- Hallgrímsson B, Jammiczky H, Young NM, Rolian C, Parsons TE, Boughner JC, Marcucio RS. 2009. Deciphering the palimpsest: studying the relationship between morphological integration and phenotypic covariation. *Evol Biol* 36:355-376. doi:10.1007/s11692-009-9076-5
- Hallgrímsson B, Lieberman DE. 2008. Mouse models and the evolutionary developmental biology of the skull. *Int Comp Biol* 43:373-384. doi:10.1093/icb/icn076
- Hallgrímsson B, Lieberman DE, Liu W, Ford-Hutchinson AF, Jirik FR. 2007. Epigenetic interactions and the structure of phenotypic variation in the cranium. *Evol Dev* 9:76-91. doi:10.1111/j.1525-142X.2006.00139.x
- Helms JA, Cordero D, Tapadia MD. 2005. New insights into craniofacial morphogenesis. *Development* 132:851-861. doi:10.1242/dev.01705
- Hill CA, Martínez-Abadías N, Motch SM, Austin JR, Wang Y, Jabs EW, Richtsmeier JT, Aldridge K. 2013. Postnatal brain and skull growth in an Apert syndrome mouse model. *Am J Med Genet A* 161A:745-757. doi:10.1002/ajmg.a.35805
- Klingenberg CP. 2009. Morphometric integration and modularity in configurations of landmarks: tools for evaluating a priori hypotheses. *Evol Dev* 11:405-421. doi:10.1111/j.1525-142X.2009.00347.x
- Klingenberg CP. 2013. Visualizations in geometric morphometrics: how to read and how to make graphs showing shape changes. *Hystrix* 24:15-24. doi:10.4404/hystrix-24.1-7691
- Klingenberg CP, McIntyre GS. 1998. Geometric morphometrics of developmental instability: analyzing patterns of fluctuating asymmetry with Procrustes methods. *Evolution* 52:1363-1375.
- Marcucio RS, Young NM, Hu D, Hallgrímsson B. 2011. Mechanisms that underlie co-variation of the brain and face. *Genesis* 49:177-189. doi:10.1002/dvg.20710
- Marroig G, Shirai LT, Porto A, de Oliveira FB, De Conto V. 2009. The evolution of modularity in the mammalian skull II: evolutionary consequences. *Evol Biol* 36:136-148. doi:10.1007/s11692-009-9051-1
- Martínez-Abadías N, Esparza M, Sjøvold T, González-José R, Santos M, Hernández M, Klingenberg CP. 2012. Pervasive genetic integration directs the evolution of human skull shape. *Evolution* 66:10-23. doi:10.5061/dryad.12g3c7ht
- Martínez-Abadías N, Heuzé Y, Wang Y, Jabs EW, Aldridge K, Richtsmeier JT. 2011. FGF/FGFR signaling coordinates skull development by modulating magnitude of morphological integration: evidence from Apert syndrome mouse models. *PLoS One* 6:e26425. doi:10.1371/journal.pone.0026425
- Metscher BD. 2009. MicroCT for developmental biology: a versatile tool for high-contrast 3D imaging at histological resolutions. *Dev Dyn* 238:632-640. doi:10.1002/dvdy.21857
- Mitteroecker P, Bookstein F. 2008. The evolutionary role of modularity and integration in the hominoid cranium. *Evolution* 62:943-958. doi:10.1111/j.1558-5646.2008.00321.x
- Mitteroecker P, Bookstein FL. 2009. The ontogenetic trajectory of the phenotypic covariance matrix, with examples from craniofacial shape in rats and humans. *Evolution* 63:727-737. doi:10.1111/j.1558-5646.2008.00587.x
- Monteiro LR. 1999. Multivariate regression models and

- geometric morphometrics: the search for causal factors in the analysis of shape. *Syst Biol* 48:192-199.
- Morimoto K, Nishikuni K, Hirano S, Takemoto O, Futagi Y. 2003. Quantitative follow-up analysis by computed tomographic imaging in neonatal hydrocephalus. *Pediatr Neurol* 29:435-439. doi:10.1016/S0887-8994(03)00401-6
- Moss ML, Young RW. 1960. A functional approach to craniology. *Am J Phys Anthropol* 18:281-291.
- Neubauer S, Gunz P, Hublin JJ. 2010. Endocranial shape changes during growth in chimpanzees and humans: a morphometric analysis of unique and shared aspects. *J Hum Evol* 59:555-566. doi:10.1016/j.jhevol.2010.06.011
- Nieman BJ, Blank MC, Roman BB, Henkelman RM, Millen KJ. 2012. If the skull fits: magnetic resonance imaging and microcomputed tomography for combined analysis of brain and skull phenotypes in the mouse. *Physiol Genomics* 44:992-1002. doi:10.1152/physiolgenomics.00093.2012
- La Merrill M, Harper R, Birbaum LS, Cardiff RD, Threadgill DW. 2010. Maternal dioxin exposure combined with a diet high in fat increases mammary cancer incidence in mice. *Environ Health Perspect* 118:596-601. doi:10.1289/ehp.0901047
- Lieberman DE, Hallgrímsson B, Liu W, Parsons TE, Janniczky H. 2008. Spatial packing, cranial base angulation, and craniofacial shape variation in the mammalian skull: testing a new model using mice. *J Anat* 212:720-735. doi:10.1111/j.1469-7580.2008.00900.x
- Opperman LA. 2000. Cranial sutures as intramembranous bone growth sites. *Dev Dyn* 219:472-485. doi:10.1002/1097-0177(2000)9999:9999<::AID-DVDY1073>3.0.CO;2-F
- Oyhenart EE, Sobrero MS, Pucciarelli HM. 1994. Heredity, nutrition and craniofacial differentiation in weanling rats: A multivariate analysis. *Am J Hum Biol* 6:277-282. doi:10.1002/ajhb.1310060302
- Polanski JM, Franciscus RG. 2006. Patterns of craniofacial integration in extant Homo, Pan, and Gorilla. *Am J Phys Anthropol* 131:38-49. doi:10.1002/ajpa.2042
- Pucciarelli HM. 1991. Nutrición y morfogénesis craneofacial. Una contribución de la Antropología Biológica Experimental. *Rev Arg Antrop Biol* 10:7-19.
- Pucciarelli HM, Goya RG. 1983. Effects of post-weaning malnutrition on the weight of the head components in rats. *Acta Anat* 115:231-237.
- Pucciarelli HM, Oyhenart EE. 1987. Effects of maternal food restriction during lactation on craniofacial growth in weanling rats. *Am J Phys Anthropol* 72:67-75. doi:10.1002/ajpa.1330720109
- Radloff DR, Rinella ES, Threadgill DW. 2009. Modeling cancer patient populations in mice: complex genetic and environmental factors. *Drug Discov Today Dis Models* 4:83-88.
- Richtsmeier JT, Aldridge K, DeLeon VB, Panchal J, Kane AA, Marsh JL, Yan P, Cole TM. 2006. Phenotypic integration of neurocranium and brain. *J Exp Zool* 306B:360-378. doi:10.1002/jez.b
- Richtsmeier JT, Flaherty K. 2013. Hand in glove: brain and skull in development and dysmorphogenesis. *Acta Neuropathol*. 125:469-489. doi:10.1007/s00401-013-1104-y
- Rohlf FJ, Corti M. 2000. Use of two-block partial least-squares to study covariation in shape. *Syst Biol* 49:740-53. doi:10.1080/106351500750049806
- Rohlf FJ, Slice DE. 1990. Extensions of the Procrustes method for the optimal superimposition of landmarks. *Syst Zool* 39:40-59. doi:10.2307/2992207
- Singh N, Harvati K, Hublin J-J, Klingenberg CP. 2012. Morphological evolution through integration: a quantitative study of cranial integration in Homo, Pan, Gorilla and Pongo. *J Hum Evol* 62:155-164. doi:10.1016/j.jhevol.2011.11.00
- Shingleton, A.W., Estep, C.M., Driscoll, M.V., Dworkin, I. 2009. Many ways to be small: Different environmental regulators of size generate different scaling relationships in *Drosophila melanogaster*. *Proc Biol Sci* 276: 2625-2633. doi:10.1098/rspb.2008.1796
- Sperber GH. 2001. Craniofacial development. London: BC Decker Inc.
- Tapiada MD, Cordero DR, Helms JA. 2005. It's all in your head: new insights into craniofacial development and deformation. *J Anat* 207:461-477. doi:10.1111/j.1469-7580.2005.00484.x
- Wiley DF, Amenta N, Alcantara DA, Ghosh D, Kil YJ, Delson E, Harcourt-Smith W, Rohlf FJ, St John K, Hamann B. 2005. Evolutionary morphing. *Proceedings of the IEEE Visualization 2005 (VIS'05)* 431-438.
- Zelditch ML, Lundrigan BL, Sheets DH, Garland T. 2003. Do precocial mammals develop at a faster rate? A comparison of rates of skull development in *Sigmodon fulviventer* and *Mus musculus domesticus*. *J Evolution Biol* 16:708-720. doi:10.1046/j.1420-9101.2003.00568.x1